KIT

Karlsruhe Institute of Technology

Dynamically Stable Walking For Humanoid Bipedal Robots Based On Walking Patterns

Bachelors's Thesis
of

Patrick Niklaus

At the Department of Informatics
Institute for Anthropomatics and Robotics (IAR)
High Perfomance Humanoid Technologies Lab (H^{2}T)

Advisor: Dr. Júlia Borràs Sol

Duration: 1. April 2014 – 1. Oktober 2014

Contents

1 Introduction

motivation, and a bit of overview of humanoid walking. I recommend to leave it for later, start with the sections that you feel its easier to write (usually, the ones that have more content).

- motivation:
    - navigating in human environments
- walking in humans:
    - CoM movement, gait phases, differences to what we do here
- static vs. dynamic walking
- overview of models used for dynamic walking

2 Models for humanoid walking

2.1 The Linear Inverted Pendulum Model

A simple model for describing the dynamics of a bipedal robot during single support phase is the 3D inverted pendulum. We reduce the body of the robot to a point-mass at the center of mass and replace the support leg by a mass-less telescopic leg which is fixed at a point on the supporting foot. Initially this will yield non-linear equations that will be hard to control. Howevery by constraining the movement of the inverted pendulum to a fixed plane, we can derive a linear dynamic system. This model called the 3D *linear* inverted pendulum model (short *3D-LIPM*).

2.1.1 The inverted pendulum

To describe the dynamics of the inverted pendulum we are mainly interested in the effect a given actuator torque has on the movement of the pendulum.

For simplicity we assume that the base of the pendulum is fixed at the origin of the current cartesian coordinate system. Thus we can describe the position inverted pendulum by a vector $c = (x, y, z)$. We are going to introduce an appropriate (generalized) coordinate system $q = (\theta_R, \theta_P, r)$ to get an easy description of our actuator torques: Let m be the mass of the pendulum and r the length of the telescopic leg. θ_P and θ_R describe the corresponding roll and pitch angles of the pose of the pendulum.

Now we need to find a mapping between forces in the cartesian coordinate system and the generalized forces (the actuator torques). Let $\Phi : \mathbb{R}^3 \longrightarrow \mathbb{R}^3, (\theta_R, \theta_P, r) \mapsto (x, y, z)$ be a function that maps the generalized coordinates to the cartesian coordinates. Then the jacobian $J_\Phi = \frac{\partial p}{\partial q}$ maps the *generalized velocites* to *cartesian velocites*. Furthermore we know that the transpose J_Φ^T maps *cartesian forces* $F = m(\ddot{x}, \ddot{y}, \ddot{z})$ to *generalized forces* (τ_r, τ_p, f).

Figure 2.1: The 3D-LIMP

We write x, y and z in terms of our generalized coordinates to compute the corresponding jacobian J_Φ. From the fact that the θ_P is the angle between the projection of c onto the xz-plane and c and θ_R the angle

between c and the projection onto the yz plane we can derive the following equations :

$$
\begin{aligned}
x &= r \cdot \sin \theta_P & &=: r \cdot s_P \\
y &= -r \cdot \sin \theta_R & &=: -r \cdot s_R \\
z &= \sqrt{r^2 - x^2 - y^2} = r \cdot \sqrt{1 - s_P^2 - s_R^2}
\end{aligned}
\tag{2.1}
$$

From which we can compute the jacobian by partial derivation:

$$
J = \frac{\partial p}{\partial q} = \begin{pmatrix}
0 & r \cdot c_P & s_P \\
-r \cdot c_R & 0 & s_P \\
\frac{2 \cdot r \cdot s_P c_P}{\sqrt{1 - s_P^2 - s_R^2}} & \frac{2 \cdot r \cdot s_R c_R}{\sqrt{1 - s_P^2 - s_R^2}} & \sqrt{1 - s_P^2 - s_R^2}
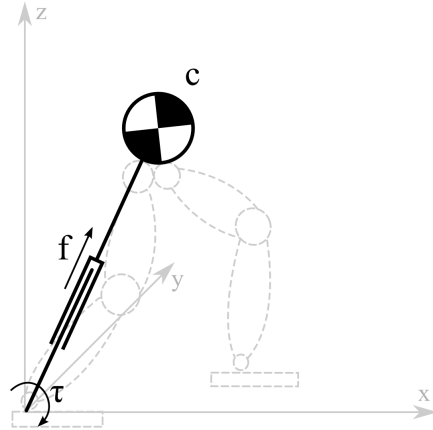\end{pmatrix}
\tag{2.2}
$$

Using the equation of motion as given by

$$
\begin{aligned}
F &= & (J^T)^{-1}\Gamma + f_g \\
m \cdot \begin{pmatrix} \ddot{x} \\ \ddot{y} \\ \ddot{z} \end{pmatrix} &= (J^T)^{-1} \begin{pmatrix} \tau_R \\ \tau_P \\ f \end{pmatrix} + \begin{pmatrix} 0 \\ 0 \\ -m \cdot g \end{pmatrix}
\end{aligned} \tag{2.3}
$$

and equations 2.2 and 2.1 we can derive the following equations:

$$
m(-z\ddot{y} + y\ddot{z}) = \frac{\sqrt{1 - s_P^2 - s_R^2}}{c_R} \cdot \tau_R + mgy \tag{2.4}
$$

$$
m(z\ddot{x} - x\ddot{z}) = \frac{\sqrt{1 - s_P^2 - s_R^2}}{c_P} \cdot \tau_P + mgx \tag{2.5}
$$

Observe that the terms of the left-hand side are not linear. To remove that non-linearity we are going to use the *linear* inverted pendulum model.

2.1.2 Linearization

In a man-made environment it is fair to assume that the ground a robot will walk on can be approximate by a slightly sloped plane. In most cases it can even assumed that there is no slope at all.

The basic assumption in the next section will be that the CoM will have a *constant displacement* with regard to our ground plane. Thus we can constrain the movement of the CoM to a plane that is parallel to the ground plane. Note that this assumption is, depending on the walking speed, only approximately true for human walking as shown by Orendurff et. al. For slow to fast walking (0.7 m/s and 1.6 m/s respectively) the average displacement in *z*-direction was found to be between 2.7*cm* and 4.81 cm. While the walking patterns generated based on the LIP-model will guarantee dynamic stability, they might not look natural with regard to human walking.

cite Orendurff

We are going to constrain the *z* coordinate of our inverted pendulum to a plane with normal vector $(k_x, k_y, -1)$ and *z*-displacement z_c:

$$
z = k_x \cdot x + k_y \cdot y + z_c \tag{2.6}
$$

Subsequently the second derivative of *z* can be described by:

$$
\ddot{z} = k_x \cdot \ddot{x} + k_y \cdot \ddot{y} \tag{2.7}
$$

Substituing 2.6 and 2.7 into the equations 2.4 and 2.5 yields the following equations:

$$
\ddot{y} = \frac{g}{z_c}y - \frac{k_x}{z_c}(x\ddot{y} - \ddot{x}y) - mz_c \cdot \tau_R \cdot \frac{\sqrt{1 - s_P^2 - s_R^2}}{c_R} \tag{2.8}
$$

$$
\ddot{x} = \frac{g}{z_c}x + \frac{k_y}{z_c}(x\ddot{y} - \ddot{x}y) + mz_c \cdot \tau_P \cdot \frac{\sqrt{1 - s_P^2 - s_R^2}}{c_P} \tag{2.9}
$$

The term $x\ddot{y} - \ddot{x}y$ that is part of both equations is still causing the equations to be non-linear. To make this equations linear we will assume that our ground plane has no slope, thus $k_x = k_y = 0$ and the non-linear terms will vanish.

Another problem is that the actuator torques τ_R and τ_P both have non-linear factors $\frac{\sqrt{1 - s_P^2 - s_R^2}}{c_R}$ and $\frac{\sqrt{1 - s_P^2 - s_R^2}}{c_P}$ respectively. This can be solved by substituting with the following *virtual inputs*:

$$\tau_P \cdot \frac{\sqrt{1 - s_P^2 - s_R^2}}{c_P} = u_P \tag{2.10}$$

$$\tau_R \cdot \frac{\sqrt{1 - s_P^2 - s_R^2}}{c_R} = u_R \tag{2.11}$$

Which yields our final description of the dynamics:

> include pattern generation just based on 3D-LIPM, I don't understand how they derived the controller

$$\ddot{y} = \frac{g}{z_c} y - \frac{u_R}{m z_c} \tag{2.12}$$

$$\ddot{x} = \frac{g}{z_c} x + \frac{u_R}{m z_c} \tag{2.13}$$

2.2 The Zero Moment Point

A very popular approach to humanoid walking are schemes based on the Zero Moment Point. One reason for that might be that it is very simple to describe constrains for dynamic stability using this reference point. As long as the following condition is met we will have full ground contact of our support foot and thus can realize dynamically stable walking: *The ZMP is strictly inside the support polygone of the support foot.*

For flat ground contact of our support foot with the floor the ZMP corresponds with the position of the center of pressure (CoP). Indeed, some author (notably Pratt) prefer to use the term CoP instead of ZMP.

The CoP of an object in contact with the ground can be computed as the sum of all contact points $p_1, \ldots, p_n$ weighted by the forces in z-direction $f_{1z}, \ldots, f_{nz}$ that is applied:

$$p := \frac{\sum_{i=1}^{N} p_i f_{iz}}{\sum_{i=1}^{N} f_{iz}} \tag{2.14}$$

An important fact (and the origin of its name) is that there are no torques around the x and y axis at the ZMP:

$$\tau = \sum_{i=1}^{N} (p_i - p) \times f_i \tag{2.15}$$

Splitting that up into each component using the definition of the cross product yields:

$$\tau_x = \sum_{i=1}^{N} (p_{iy} - p_y) f_{iz} - \overbrace{(p_{iz} - p_z)}^{=0} f_{iy} \tag{2.16}$$

$$\tau_y = \sum_{i=1}^{N} \overbrace{(p_{iz} - p_z)}^{=0} f_{ix} - (p_{ix} - p_x) f_{iz} \tag{2.17}$$

$$\tau_z = \sum_{i=1}^{N} (p_{ix} - p_x) f_{iy} - (p_{iy} - p_y) f_{ix} \tag{2.18}$$

Since we have flat ground contact, all contact points have the same z-coordinate as the ZMP, thus we can simplify τ_x and τ_y to:

$$\tau_x = \sum_{i=1}^{N} (p_{iy} - p_y) f_{iz} = \sum_{i=1}^{N} (p_{iy} f_{iz}) - (\sum_{i=0}^{N} f_{iz}) \cdot p_y \tag{2.19}$$

$$\tau_y = \sum_{i=1}^{N} -(p_{ix} - p_x)f_{iz} = \sum_{i=1}^{N} -(p_{ix}f_{iz}) + (\sum_{i=0}^{N} f_{iz}) \cdot p_x \tag{2.20}$$

Furthermore we can use the corresponding components p_x and p_y from the definition of the ZMP 2.14 and substitude in the equations 2.19 and 2.20.

This will yield: $\tau_x = \tau_y = 0$.

Please note that τ_z will in general not be zero, nonetheless in case of straight walking it is often assumed to be zero as well.

2.3 The table-cart model

The table-cart model is equivalent to the 3D-LIPM model discussed before, but somewhat more intuitive for computing the resulting ZMP from an CoM motion. The model consists of an (infinitely) large mass-less table of height z_c, while the foot of the table has the shape of the support polygone. Given a frictionless cart with mass m that moves on the table we can compute the resulting ZMP in the support foot. Please note that the 3D-dimensional model is equivalent to having two independent tables with two carts each in the xz and yz-plane respectively. First of all, lets compute the torque τ_x and τ_y around the x-axis and y-axis at the ZMP on the support foot.

$$\tau_y = \overbrace{-mg(c_x - p_x)}^{\text{torque due to gravity}} + \overbrace{m\ddot{x} \cdot z_c}^{\text{torque due to acceleration of cart}} \tag{2.21}$$

$$\tau_x = -mg(c_y - p_y) + m\ddot{y} \cdot z_c \tag{2.22}$$

Please note the similarity to the equations 2.12 and 2.13 when assuming the base of the pendulum is located at p. If we now use the property of the ZMP that the torque around the x and y-axis is zero, we can solve for the ZMP position p:

$$p_x = c_x - \frac{z_c}{g}\ddot{c}_x \tag{2.23}$$

$$p_y = c_y - \frac{z_c}{g}\ddot{c}_y \tag{2.24}$$

2.4 Multi-Body methode to calculate the ZMP

Besides the simplified table-cart model, there also exsists an exact methode to calculate the resulting ZMP from the movement from serveral connected rigid bodies.

Let c_i be the CoM position and m_i the mass of the i-th body ($i \in \{1, ..., k\}$). Then the total linear momentum $\mathscr{P}$ can be calculated by:

$$\mathscr{P} = \sum_{j=1}^{k} m_j \cdot \dot{c}_j \tag{2.25}$$

If ω_i the angular momentum and R_i is the rotational part of the reference frame of the i-th body and I_i the inertia tensor in that reference frame, the total angular momentum $\mathscr{L}$ can be calculated by:

$$\mathscr{L} = \sum_{j=1}^{k} c_j \times (m_j \dot{c}_j) + R_j I_j R_j^T \omega_j \tag{2.26}$$

If we denote the total mass of the robot with M and the gravity vector with g we can express the change of linear momentum if a force f is applied to the body as:
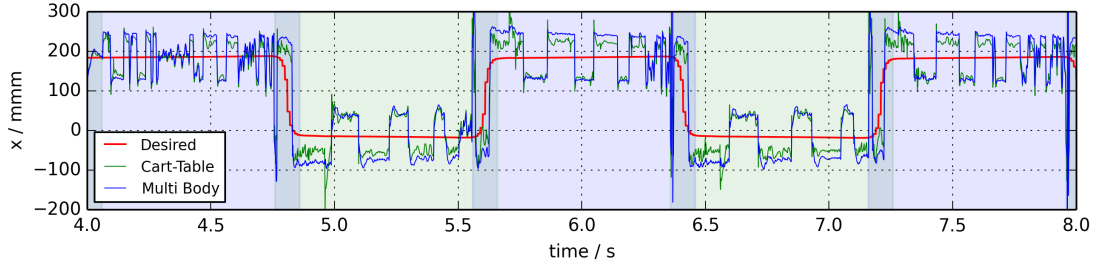
Figure 2.2: Comparision of the Cart-Table and Multi-Body to estimate the realized ZMP during walking.

$$\dot{\mathscr{P}} = Mg + f \tag{2.27}$$

And subsequently the change in angular momentum if a torque τ is applied:

$$\dot{\mathscr{L}} = c \times Mg + \tau \tag{2.28}$$

To calculate the resulting torque τ_{ZMP} around the ZMP located at p we can use:

$$\tau_{ZMP} = \tau + (0 - p) \times f = \tau - p \times f \tag{2.29}$$

If solve equation 2.27 for f and 2.28 for τ and substitute them in 2.29 this yields the following equation:

$$\tau_{ZMP} = \dot{\mathscr{L}} - c \times Mg - p \times (\dot{\mathscr{P}} - Mg) \tag{2.30}$$

Since we know that the torque around the ZMP is zero around the x and y axis we can apply the definition of the cross product and solve for the ZMP position:

$$p_x = \frac{Mgx + p_z \dot{\mathscr{P}}_x - \dot{\mathscr{L}}_y}{Mg + \dot{\mathscr{P}}_z} \tag{2.31}$$

$$p_y = \frac{Mgy + p_z \dot{\mathscr{P}}_y - \dot{\mathscr{L}}_x}{Mg + \dot{\mathscr{P}}_z} \tag{2.32}$$

Both equations are dependent on p_z. If we assume the robot walks on a flat floor, we can set $p_z = 0$.

See figure **??** to get an idea how much the Multi-Body ZMP derives from the estimation using the Cart-Table model.

2.5 Simulating rigid body dynamics

For physical simulation in general can be devided into discrete methodes and continous methodes. Discrete simulators only compute the state of the system at specific points in time, while continous simulators are able to compute the state of the system at any point in time. While contious simulation is the more flexible approach, it quickly becomes impractical with the number of constrains involved. Typically a large amount of differential equations need to be solved. Since it is hard to obtain analytical solutions for most differential equations, numerical methods need to be used, which often have a large runtime. On contrast discrete simulation methods only compute simulation values for specific time steps. This exploits the observation that we will typically query the state of the physics engine only at a fixed rate anyway, e.g. at each iteration of our control loop). Rather than solving the differntial equations that describe the physical system in each step, a solution is derived from the previous simulation state.

A physical system we can typically find two kind of forces: Applied forces and constraint forces. Applied forces are the input forces of the system. Source of applied forces are for example objects like springs or gravity. Constraint forces are fictious forces that arrise from contrains we impose on the system: Non-penetration constraints, friction constraints, position constrains of joints or velocity constrains for motors. Mathematically we can express such constrains in the form: $C(x) = 0$ or $\dot{C}(x) = 0$ in the case of equality constrains, or as $C(x) \geq 0$ or $\dot{C}(x) \geq 0$ in the case of inequality constrains. For example the position constraint of a joint p connected to a base p_0 with distance $r_0 = ||p - p_0||$ would be: $C(p) = ||p - p_0||^2 - r_0^2$ If p is moving with a linear velocity v a constraint force F_c is applied to p to maintain this constraint. We can view C as a transformation from our cartesian space to the constraint space. Thus by computing the jacobian J of C we can relate velocities in both spaces. Furthermore we can realte constraint space forces λ with cartesian space forces using the transpose of the Jacobian. Thus if we can find the constraint space force λ that is needed to maintain this constraint we can compute F_c using $F_c = J^T \lambda$. Computing this constraint space forces is the task of the constraint solver.

The constrained solver used by BULLET and thus the constraint solver used for simulating the patterns here is a sequential impulse solver. To make some calculations easier, a SI solver works with impulses and velocities rather than forces and accelerations. Impulses and forces can be easily transformed in eachother as $P = F \cdot T$ where P is the impulse and T the timestep size. A sequential impulse solver tries to compute the constraint force (in this case rather impulse) λ for each costraint *seperately*. For each constraint the following steps are executed:

1. Compute the velocity that results from *applied forces* on the body
2. Calculate constraint force to satisfy the velocity constraint
3. Compute new velocity resulting from constraint force *and* applied force on the body
4. Update position of the body by integrating velocity: $p[n+1] = p[n] + v \cdot T$

Of course this might not lead to a global solution, as satisfying a constraint might violate a previously solved one. The idea is to repeadidetly loop over all constraints, so that a global solution will be reached. Obviously the quality of this methode relies on how often this loop is executed. Consider the case of a kinematic chain where a movement of a link always violates at least one constraint. It is clear that this methode needs a lot of iterations to yield good results in this case. It becomes even worse in the case of a parallel kinematic that is in contact with the ground, as is the case for a bipedal robot in dual support stance. Solving a non-penetration constrain on either end, will invalidate the position constraint of the next link. In turn, the position constraint of each link needs to be updated until the other end of the kinematic chain is reached. If the non-penetration constraint is violated again for this end, the whole process starts again in reverse direction. This leads to oscillations that need a lot more iterations to level off to an acceptable level. Dispite these inaccuracies using enought solver iteration this still yields an overall usable systems. However the velocities still will have a small random error in each simulation step. This poses a major problem when trying to measure accelerations, as the random error acauses them to accelerate wildly. This circumstance needs to be taken into account when dealing with values derived from the acceleration (e.g. the ZMP), as mean-filters might be neccessary.

3 Pattern generator

To generate a walking pattern for a bipedal robot two basic approaches are common:

1. Generate (or modify) foot trajectories that realize a prescribed trajectory of the CoM

2. Generate a CoM trajectory for prescribed foot trajectories

The first approach is generally used for implementing pattern generators soley based on the 3D-LIPM model.

citation needed

The second approach is the more versatile one, since it is easy to incorporate constrains of our environment (e.g. only limited foot holds) in the input of the pattern generator. However care must be taken while chosing adequate step width and step length parameters for the foot trajectory, so that they can actually be realized by the robot.

add citation

The pattern generator proposed by Kajita et al. based on Preview Control realizes the second approach. We will discuss the theoretical background of this pattern generator here in more detail, since all pattern that we used where generated that way.

3.1 Computing the CoM from a reference ZMP

As we saw in the section 2.3 it is easy to compute the resulting ZMP given the CoM and its acceleration. However for generating the walking pattern, we want to compute the CoM trajectory from a given ZMP. If you rearange the equations 2.23 and 2.24 you see that we have to solve a second order differential equations:

$$c_x = \frac{z_c}{g} \cdot \ddot{c}_x + p_x \tag{3.1}$$

$$c_y = \frac{z_c}{g} \cdot \ddot{c}_y + p_y \tag{3.2}$$

There are several ways to solve this differential equations, for example by transforming them to the frequency-domain. This however would mean, the ZMP trajectory needs to be transformed to the frequency domain as well, e.g. using Fast Fourier Transformation. This has two main problems:

1. It has a significant computational overhead. (For FFT the additional runtime would be in $O(n \log n)$)

2. We need to know the whole ZMP trajectory in advance.

Instead Kajita et. al. chose to define a dynamic system in the time domain that describes the CoM movement.

maybe do a formal introduction into dynamic system and the state space approach

3.1.1 Pattern generation as dynamic system

For simplicity we will only focus on the dynamic description of one dimension, as the other one is analogous. To transform the equations to a strictly proper dynamical system, we need to determine the state vector of our system. For the table-cart model it suffices to know the position, velocity and acceleration of the cart. Thus the state-vector is defined as $x = (c_x, \dot{c}_x, \ddot{c}_x)$. We can define the evolution of the state vector as follows:

$$\frac{d}{dt}\begin{pmatrix} c_x \\ \dot{c}_x \\ \ddot{c}_x \end{pmatrix} = \overbrace{\begin{pmatrix} 0 & 1 & 0 \\ 0 & 0 & 1 \\ 0 & 0 & 0 \end{pmatrix}}^{=:A_0} \cdot \begin{pmatrix} c_x \\ \dot{c}_x \\ \ddot{c}_x \end{pmatrix} + \overbrace{\begin{pmatrix} 0 & 0 & 0 \\ 0 & 0 & 0 \\ 1 & 0 & 0 \end{pmatrix}}^{=:B_0} u \tag{3.3}$$

As you can see the jerk of the CoM was introduced as an input $u_x = \frac{d}{dt}\ddot{c}_x$ into the dynamic system.

We use equation 2.23 to calculate the actual output of the dynamic system the resulting zmp, that will be controlled:

$$p_x = \begin{pmatrix} 1 & 0 & \frac{-z_c}{g} \end{pmatrix} \cdot \begin{pmatrix} c_x \\ \dot{c}_x \\ \ddot{c}_x \end{pmatrix} \tag{3.4}$$

Using this formulation of the dynamic system we need to derive the evolution of our state vector using the state-transition matrix. Since our input ZMP trajectory will consist of discrete samples at equal time intervals T we define the discrete state as $x[k] := x(k \cdot T)$. Please note that this system is a linear time-invariant system (LTI), and both matrices A_0 and B_0 are constant. We can therefore use the standart approach to solve this system using the equation:

$$x(t) = e^{A_0 \cdot (t-\tau)} x(\tau) + \int_\tau^t e^{A_0 \cdot (t-\lambda)} B_0 u(\lambda) d\lambda \tag{3.5}$$

In our discrete case that becomes:

$$\begin{aligned} x[k+1] &= e^{A_0 \cdot ((k+1)T - kT)} x[k] + \int_{kT}^{(k+1)T} e^{A_0 \cdot ((k+1)T - \lambda)} B_0 u(\lambda) d\lambda \tag{3.6} \\ &= e^{A_0 \cdot T} x[k] + \left(\int_{kT}^{(k+1)T} e^{A_0 \cdot ((k+1)T - \lambda)} d\lambda \right) \cdot B_0 u[k] \tag{3.7} \\ &= e^{A_0 \cdot T} x[k] + \left(\int_T^0 e^{A_0 \cdot \lambda} d\lambda \right) \cdot B_0 u[k] \tag{3.8} \end{aligned}$$

Keep in mind that $u(\lambda) = u[k], \lambda \in (kT, (k+1)T)$ so we can move it outside of the integral. Let us first compute a general solution for the matrix exponential $e^{A_0 \cdot t}$. It is easy to see that A_0 is nilpotent and $A_0^3 = 0$, thus the computation simpilfies to the following:

$$e^{A_0 t} := \sum_{i=0}^{\infty} \frac{(A_0 \cdot t)^i}{i!} = I + A_0 \cdot t + A_0^2 \cdot \frac{t^2}{2} + 0 = \begin{pmatrix} 1 & t & \frac{t^2}{2} \\ 0 & 1 & t \\ 0 & 0 & 1 \end{pmatrix} \tag{3.9}$$

Using this solution computing the integral in 3.6 is quite easy:

$$\int_T^0 e^{A_0 \cdot \lambda} d\lambda = -\int_0^T \begin{pmatrix} 1 & t & \frac{t^2}{2} \\ 0 & 1 & t \\ 0 & 0 & 1 \end{pmatrix} dt = - \begin{pmatrix} t & \frac{t^2}{2} & \frac{t^3}{6} \\ 0 & t & \frac{t^2}{2} \\ 0 & 0 & t \end{pmatrix} \Bigg|_0^T = \begin{pmatrix} T & \frac{t^2}{2} & \frac{T^3}{6} \\ 0 & T & \frac{T^2}{2} \\ 0 & 0 & T \end{pmatrix} \tag{3.10}$$

Substituting the results in 3.6 yields:

$$x[k+1] = \overbrace{\begin{pmatrix} T & \frac{t^2}{2} & \frac{T^3}{6} \\ 0 & T & \frac{T^2}{2} \\ 0 & 0 & T \end{pmatrix}}^{=:A} x[k] + \overbrace{\begin{pmatrix} \frac{T^3}{6} \\ \frac{T^2}{2} \\ T \end{pmatrix}}^{=:B} \cdot u_x[k] \tag{3.11}$$

3.1.2 Controlling the dynamic system

To control this dynamic system we need to determine an adequate control input u_x to realize the reference ZMP trajectory. A performance index J_x for a given control input u_x is needed to formalize what a "good" control input would be. A naive performance index could be:

$$J_x[k+1] := (p_x^{ref}[k+1] - p_x[k+1])^2 \tag{3.12}$$

To minimize it, we need to find u_x for which $p_x = p_x^{ref}$. By substituting $p_x[k+1]$ with 3.4 and $x[k+1]$ with 3.11 this yields:

$$u_x[k] = \frac{p_x^{ref}[k+1] - C \cdot A \cdot x[k]}{C \cdot B} = \frac{p_x^{ref}[k+1] - (1, T, \frac{1}{2}T^2 - \frac{z_c}{g}) \cdot x[k]}{\frac{1}{6}T^3 - \frac{z_c}{g}T} = \frac{p_x^{ref}[k+1] - p_x[k] - T\dot{c}_x[k] - \frac{1}{2}T^2\ddot{c}_x[k]}{\frac{1}{6}T^3 - \frac{z_c}{g}T} \tag{3.13}$$

insert plot To analyse the behaviour of this control law for u_x we simulate the rapid change of reference ZMP when changing the support foot.

As you can see the reference ZMP is perfectly tracked. However, the CoM does not behave as expected. To achive the required ZMP position the CoM will be *accelerated indefinietly* in the opposite direction. Clearly this is not desired and will lead to falling on a real robot. A more sophisticated performance index is needed. To eventually reach a stable state at which the CoM comes to rest, the performance index should include a state feedback. Also note the large jerk that is applied to the system when the reference ZMP position changes rappidly. In a real mechanical system large jerks will lead to oszillations, which will disturb the system. Thus the performance index should also try to limit the applied jerk.

Another problem is caused by the very nature of a controller: The controller starts to act *after* we have a deviation from our reference ZMP trajectory. Trying make this lag as small as possible can lead to very high velocities, which might not be realizable by motors of a robot. However we have at least limited knowledge of the future reference trajectory. This knowledge can be leveraged by using Preview Control, add citation katayama which considers the next N timesteps for computing the performance index.

Kajita et. al. use a performance index proposed by Katayama et. al. to solve all of the problems above:

$$J_x[k] = \sum_{i=k}^{\infty} Q_e e[i]^2 + \Delta x[i]^T Q_x \Delta x[i] + R\Delta u_x[i]^2 \tag{3.14}$$

Q_e is the error gain, Q_x a symmetric non-negative definite matrix (typically just a diagonal matrix) to weight the components of $\Delta x[i]$ differently and $R > 0$. Conveniently Katayama also derived an optimal controller for this performance index, which is given by:

$$u[k] = -G_i \sum_{i=0}^{k} e[k] - G_x x[k] - \sum_{j=1}^{N} G_p p_x^{ref}[k+j] \tag{3.15}$$

The gains G_i, G_x, G_p, can be derived from the parameters of the performance index. Since the calculation is quite elaborate we refer to the cited article by Katayama p. 680 for more details.

3.2 Implementation

block diagramm of architechture To generate walking patterns based on the ZMP preview control methode, the approach from Kajita was implemented in LIBBIPEDAL a shared library. A front-end was developed to easily change parameters, visualize and subsequently export the trajectory to the MMM format. The implementation was build on a previous implementation, which was refactored, extended and tuned with respect to results from the dynamics simulation.

The pattern generator makes extensive usage of SIMOX VIRTUALROBOT, for providing a model of the robot and the associated task of computing the forward- and inverse kinematics.

Generating a walking pattern consists of multiple steps. First the foot positions are calculated. These are used to derive the reference ZMP trajectory which is feed into the zmp preview controller. From that the CoM trajectory is computed. The CoM trajectory and feet trajectories are then used to compute the inverse kinematics. The resulting joint trajectory is displayed in the visual front-end and can be exported. Each step is contained in dedicated modules that can be easily replaced, if needed. We will outline the implementation of each module seperately.

3.2.1 Generating foot trajectories

To generate the foot trajectories several parameters are needed:

table with used parameters

Step height h Maximum distance between the foot sole and the floor

Step length l Distance in anterior direction (y-Axis) between the lift-off point and the touch-down point

Step width w Distance in lateral directoin (x-Axis) between both TCP on the feet

Single support duration t_{ss} Time the weight of the robot is only support by exactly one foot

Dual support duratoin t_{ds} Time the weight of the robot is supported by both feet

Walking straight

Since the foot trajectories of a humanoid walking have a cyclic nature, we only need three different foot trajectories that can be composed to arbitrarily long trajectories: Two transient trajectories for the first and last step respectively and a cyclic motion that can be repeated indefinetly. We can use the same trajectories for both feet, as they are geometrically identical. Each foot trajectory starts with swing phase and a resting phase. The trajectory in y and z direction is computed by a 5th order polynomial that assures the velocities and accelerations are approaching zero at the lift-off and touch-down point. The first and last step only have half of the normal step length, since the trajectory is starting and ending from a dual support stance, where both feet are placed parallel to eachother. Each trajectory is encoded as a $6 \times N$ matrix, each column containing cartesian coordinates and roll, pitch and yaw angles.

Walking on a circle

Much of the general structure of the foot trajectory remains the same as for walking straight. However instead of specifing the step length, it is implicitly given by the segment of the cricle that should be traversed and the number of steps. So extra care needs to be taken to specify enough steps so that the generated foot positions are still. Each foot needs to move on a circle with radius $r_{inner} = r - \frac{w}{2}$ or $r_{outer} = r + \frac{w}{2}$ depending which foot lies in the direction of the turn. The movement in z-direction remains unaffected. However the movement in the xy-plane is transformed to follow the circle for the specific foot. The same polynomial that was previously used for the y-direction is now used to compute the angle on the corresponding circle and the x and y coordinates are calculated acordingly. The foot orientation is computed from the tangential (y-Axis) and normal (x-Axis) of circle the foot follows.

Current implementation does effectively that, but is actually a hack. Needs seperate trajectories for left/right

Balancing on one foot

To test push recovery from single support stance a special pattern was needed. To generate this another footstep planer was implemented that generates a trajectory for standing on one foot. Starting from dual support stance, the swing leg is moved in vertical direction until the usual step height is achieved. Additionally the foot is moved in lateral direction to half the step width. This reduces the necessary upper body tilt to compensate the inbalance. For the last step the inverse movement is performed to get

It is easy to extent this: DO IT.

back into dual support stance. This methode could be extended to walk by setting the next support foot in a straight line before the current support foot. The swing foot would need to be moved in an arc in lateral direction to avoid self-collisions.

3.2.2 ZMP reference generation

As an input for the ZMP preview control, we need a reference ZMP movement that corresponds with the foot trajectory. The reference generator receives a list of intervals associated with the desired support stance and foot positions as input. In single support phase, the reference generator places the ZMP in the center of the support polygone of the corresponding foot. Since the support polygone is convex, the center is the point furthest away from the border of the polygone. Thus it should guarantee a maxium of stability with regard to possible ZMP errors. In dual support phase, the reference generator shifts the ZMP from the previous support foot to the next support foot. Kajita et. al. suggest using a poylnomial to interpolate the ZMP positions between the feet. However a simple step function $\sigma(t) = \begin{cases} p_1 & t \leq t_0 \\ p_2 & t > t_0 \end{cases}$ seems to suffice as well. Since the the touch-down of the swing foot might have a small lag, it is important that t_0 is the middle of the dual support phase. This assures we do not start to move the ZMP too early.

3.2.3 ZMP Preview Control

Add timings, implement configurable preview periode

This module implements the methode described by Kajita et. al. and uses the methode outlined by Katayama et. al. to compute the optimal control input $u[k]$. Since it is computational feasable, the preview period consists of the full reference trajectory. For an online usage of this methode, this could be reduced to a much smaller sample size. Using the system dynamics described by 3.11 the CoM trajectory, velocity and acceleration can be computed. The implementation makes heavy use of Eigen, a high performance linear algebra framework that uses SIMD instructions to speed up calculations. Thus thus a calculation time of FIXME: calculation time could be achieved.

3.2.4 Inverse Kinematics

Using the foot trajectories and CoM trajectory the actual resulting joint angles need to be calculated. Since the kinematic model that is used has a total of FIXME: DOF degrees of freedom, we need to reduce the number of joints that are used to a sensible value. For walking only the joints of the legs and both the torso roll and pitch joints are used. All other joints are constrained to static values that will not cause self-collisions (e.g. the arms are slightly extended and do not touch the body). For comptuing the IK additional constraints where added, to make sure the robot has a sensible pose: The chest should always have an upright position and the pelvis should always be parallel to the floor. To support non-straight walking, the pelvis and chest orientation should also follow the walking direction. Thus the following methode to compute the desired chest and pelvis orientation is used:

1. Compute walking direction y' as normed mean of y-Axis of both feet: $y' := \frac{y_{left} + y_{right}}{|y_{left} + y_{right}|}$

2. Both should have an upright position $z' := (0, 0, 1)^T$

3. Compute x' as the normal to both vectors: $x' := y' \times z'$

4. Pose R' is given by $R' = (x', y', z')$

A special property of the model that was used for computing the inverse kinematics, is that TCP of the left leg was chosen as root node. Since we can specify the root position freely, that removes the need of solving for the left foot pose. Thus the following goals need to be satisfied by the inverse kinematics:

1. Chest orientation

2. Pelvis orientation

3. CoM position

4. Right foot pose

To solve the inverse kinematics a hiearchical solver was used to solve for that goals in the given order. It was observed that specifing a good target height for the CoM is of utmost importance for the quality of the IK. Specifing the CoM height too height or too low can lead to the effective loss of degrees of freedom.

Maybe a more theoretical explaination?

3.2.5 Trajectory Export

The trajectory was exported in open MMM trajectory format. The format was extended to export additional information useful for debugging and controlling the generated trajectory. That means besides the joint values and velocites the trajectory also includes the CoM and ZMP trajectory that was used to derive them. Also information about the current support phase is saved. For convinience the pose of chest, pelvis, left and right foot are exported as homogenous matrices as well. This was done to save the additional step of computing them again from the exported joint trajectory for the stabilizer and also reduce an additional error source.

Maybe doing the FK now would be better and more versatile, since we could feed normal MMM trajectories in the stabilizer

3.3 Dynamic simulation

To evaluate the generated trajectories a simulator for the dynamics was developed. The simulator was build on the SIMDYNAMICS framework that is part of SIMOX. SIMDYNAMICS uses Bullet Physics as underlying physics framework. A big part of the work on the simulator was spend on configuring the parameters and finding flaws in the physics simulation. Thus the simulator includes a extensive logging framework that measures all important parameters of the simulation. For visulizing and analysing the measurement the Open Source tools IPYTHON, numpy and PANDAS where used.

3.3.1 Practical challenges of physics simulation

While walking only the feet of the robot are in contact with the ground. Thus the stability of the whole robots depends on the contact of the feet with the floor. Especially in single support phase that area is very small with regard to the size of the robot. For that reason the accuracy of ground contatc forces and friction is of utmost importance for the quality of the simulation. In general three classes of errors need to be elimnated to get a good simulation:

1. Incorrectly configured parameters, such as fictions coefficent and contact thresholds

2. Numerical errors

3. Inherent errors of the methode

As outline in the section about discrete time dynamic simulation, the physics of the system are formulated as input forces and constrains that need to be solved for the constraint forces. Since bullet uses an iterative approach that solves each constraint independently, it is of utmost importance to use a sufficient amount of iterations for each simulation step. Another important parameter is the timestep of each simulation step. Through experimental evaluation a simulation with 2000 solver iterations and a timestep size of 1ms was sufficiently stable. However since the number of iterations is very high and a lot of timesteps are calculated during the simulation, numeric errors become significant. That made is neccessary to enable using double precision floating point numbers for the values used during simulation.

To decide which contact constrains are active for which points, Bullet must solve for object collisions. Depending on the objects involved different algorithms are used to calculate the contact points. Major

gains in accuracy could be observed by replacing the feet and the floor with simple box shapes, instead using mesh based models.

3.3.2 Simulating walking patterns

The simulator was designed to load arbitrary motions in the MMM format and replay them. Additional stabilization algorithms can be applied depending on additional information provided in the MMM motions.

Even during simple playback of a trajectory, a number of conisderations due to the dynamics need to be taken into account. We will outline some of the problems and how they where resolved.

Simply applying the joint values at the given point in time, will lead to large jumps in velocity, acceleration and jerk. This will cause large oscillations, which in turn result in destabilizing disturbances. Interpolation between the joint angles of two frames can mitigate this. To implement this cubic splines where used instead of linear interpolation, as they also ensure that the velocity is continous.

Disturbances due to the simulation will cause position errors in the joints. To fix that PID based motor controllers were added to SIMDYNAMICS. They control the motor velocites to compensate position errors.

Since the motors used by the simulation framework are velocity controlled, their acceleration is not limited. This is not consistent with real motors, thus limits for velocites and acceleration where introduced to SIMDYNAMICS, that can be configured on a per-joint basis.

An important part of the simulation is the generation of measurements that can saved to be carefully evaluted offline or displayed in the visualization. For this purpose a modular measuremt component was added to the simulator. An important design goal was to keep the measurement component as simple to extend and maintain as possible. Each module meassures a specific set of values and writes them, indexed by the corresponding timestamp, to its log file. As output format the well know plaintext format CSV was used. The visualization can query the measurement components directly to get the newest values to be displayed. For example the ZMP module measures the actual ZMP and also provides an interface to query the trajectory ZMP and the reference ZMP that was provided as input for the pattern generator. Thus all three values can be displayed in the visualization and easily compared later by analysing the log file. Since the goal was to keep the component as simple as possible, we use exsistening well known tools for analysing the generated log files. Some small helper scripts are provied to make it easier to load the data into the time series analysis framework PANDAS. PANDAS interfaces with the popular plotting framework MATPLOTLIB to diplay plots of the data. IPYTHON is used to easily run the analysis and display the results in a browser window. All plots of simulated patterns found in this thesis can be generated automatically for every simulation.

> Make sure you can really load vanilla MMM trajectories without crashing

> Screenshot of analysis software

4 Stabilizing a trajectory

While executing a trajectory there are several sources of errors that will make it neccessary to correct the trajectory. We can devide them in about three main classes:

Disturbances of the environment: Pattern generator make some assumptions about the environment they operate in. Most prominently the 3D-LIMP assumes the floor is completely flat and has no slope. Also we assume we can navigate without colliding with other object. Any environment that deviates from this assumption can be seen as a disturbance.

Disturbances due to simulation errors: Physical simulations often make a tradeoff between speed and simulation accuracy. Thus the simulation might not always behave as it was modeled during calculating the pattern, or as it would behave in reality.

Disturbances due to errors of the methode: Often pattern generators use simplified models of the dynamics involved to derive generation scheme. For example the pattern generator that was used here assumes the ZMP behaves as the cart-table-model predicts. However the real ZMP calculated from the multi-body dynamics can substantially deviate.

4.1 Controlling a deviation

When using a ZMP based control scheme to derive a walking pattern it seems natural to check for deviations of the actual ZMP from the goal ZMP. However a deviation from the reference ZMP does not neccessarily mean we will see any disturbance. As long a the ZMP remains inside the support polygone the trajectory can be executed as planed. Also we saw before, it is entirely possible to realize the reference ZMP while being in an overall state that deviates significantly from the state we assumed while generating the pattern. Thus we also need to check for a diviation in the trajectory of our CoM. A common approach to correct for CoM position is to control the pose of the chest frame of the robot. This only works if the majority of the mass of a robot is located in the upper body and arms. Luckily for most humanoid robots this is the case.

4.2 Stabilizer

We chose a stabilizer proposed by Kajita et. al. in their 2010 paper. . The stabilizer only needs a joint trajectory of the walking pattern augmented with a desired ZMP trajectory. This allows the stabilizer to use patterns that where generated synthetically, e.g. by a pattern generator, or patterns that are the results of (adapted) motion capturing. The methode proposed by Kajita does not need a torque controlled robot, but works with position control. This was very important for the selection of this stabilizer as, the motors in BULLET are velocity controlled, thus we can not controll the torque directly.

The controller works by attaching control frames to specific points on the robot. The reference position of this frames can be calculated from the input trajectory using forwards kinematics. To compensate a disturbance the orientation of a reference frame is modified. The modified reference frames are then converted to the modified joint angles by the inverse kinematics.

In the remainder of this chapter we will use the superscript d to denote reference values and the subscript $*$ to denote modified values.

For this approach four control frames where selected. The chest to modify the body posture, the feet to modify the ankle torque, and the pelvis to modify the difference between contact forces of the two feet.

4.2.1 Controlling the body posture

The control strategy of the chest pose is straight forward: Given the reference roll angle ϕ^d and reference pitch angle θ^d compute the differences to the actual angles ϕ and θ. The main problem in a real robot is to obtain the actual global pose of this frame. The proposed methode is to use a Kalman filter to estimate the pose from the joint position and accelerometers. We did not implement this methode in simulation, as it is easy to obtain the exact pose from the simulator. To prevent rapid movements of the chest that cause large accelerations, a dampening controller is used. The angles $\Delta\phi$ and $\Delta\theta$ can be calculated by the following equations:

$$\Delta\dot{\phi} = \frac{1}{D_c}(\phi^d - \phi) - \frac{1}{T_c} \cdot \Delta\phi \tag{4.1}$$

$$\Delta\dot{\theta} = \frac{1}{D_c}(\theta^d - \theta) - \frac{1}{T_c} \cdot \Delta\theta \tag{4.2}$$

D_c describes the dampening gain. T_c is constant that describes how long it will take to reach the normal positions $\Delta\phi = 0$ and $\Delta\theta = 0$ respectively if there is no error.

The modified reference frame R_c^{d*} can the be calculated by rotating the reference frame by the additional angles:

$$R_c^{d*} = R^d \cdot R_{RPY}(\Delta\phi, \Delta\theta, 0) \tag{4.3}$$

To get an idea how this controller compensates CoM inaccuracies consider the case where the upper body is bent forward. Since our reference trajectory specifies an upright upper body pose we can assume that $\phi^d = 0$. Since the upper body is bent forward the roll angle ϕ will be below zero. Depending on D_c we will eventually reach $\Delta\phi \approx |\phi|$, thus the reference frame will be modified to bent backwards to compensate the wrong pose.

4.2.2 Controlling the ankle torques

Since the stabilizer only has the joint trajectory and desired ZMP trajectory as input, we need a way to compute the desired actuation torques on the ankles. The canonical way to do this, would be to solve the inverse dynamics of the robot. However for this we need an acurate model of the robot, including correct masses and moments of intertia for each link. This model is not always easy to obtain and calculating the inverse dynamics of a robot with many degrees of freedom is rather slow. For this reason a simple heuristic is proposed to yield approximate torques given a reference ZMP position. However in the single support phase it is easy to calculate the *exact* actuation torque on the ankle, that is required to realize the given reference ZMP.

First we need to calculate the force in z-direction applied on the foot at the ankle p_{ankle} which we name f_g by:

$$f_g = M \cdot g \tag{4.4}$$

Where g is the gravity vector and M the mass of the robot. Given f_g acting on the ankle position p_{ankle} we can obtain the ankle torque in single support phase easily using the fact, that the torque around the ZMP is zero:

$$
\begin{aligned}
\tau_{zmp} &= (p_{ankle} - p_{zmp}^d) \times f_g &+& \tau_{ankle}^d \\
0 &= (p_{ankle} - p_{zmp}^d) \times f_g &+& \tau_{ankle}^d \\
\tau_{ankle}^d &= -(p_{ankle} - p_{zmp}^d) \times f_g & &
\end{aligned}
\tag{4.5}
$$

In dual support phase however that matter is more complicated. Since both feet are in contact with the ground, the weight of the robot is distributed between them. If we take the forces f_R and f_L which act on the right ankle p_R and left ankle p_L respectively we know that $f_R + f_L = f_g$. Thus there exists $\alpha \in [0,1]$ for which: $f_R = \alpha \cdot f_g$ and $f_L = (1 - \alpha) \cdot f_g$. A heuristic for computing this alpha is the *ZMP distributor*.

The idea is to calculate the nearest points $p_{L\#}$ and $p_{R\#}$ from the ZMP to the support polygones of the feet. If the ZMP falls inside one of the support polygones set $\alpha = 1$ or $\alpha = 0$ respectively. If it is outside of bothe support polygones the ZMP is projected onto line from $p_{L\#}$ to $p_{R\#}$ yielding the point p_α.

We can then set α to:

$$\alpha = \frac{|p_\alpha - p_{L\#}|}{|p_{R\#} - p_{L\#}|} \tag{4.6}$$

If τ_L and τ_R are the torques in the left and right ankle respectively, we can calculate the torque around the ZMP as:

$$\tau_{zmp} = (p_R - p_{zmp}^d) \times f_R + (p_L - p_{zmp}^d) \times f_L + \tau_L^d + \tau_R^d \tag{4.7}$$

As before, we assume that $\tau_{zmp} = 0$ which lets us solve 4.7 for $\tau_0 := \tau_L^d + \tau_R^d$:

$$\tau_0 = (p_R - p_{zmp}^d) \times f_R + (p_L - p_{zmp}^d) \times f_L \tag{4.8}$$

We now again apply a heurstic using the α computed before to distribute τ_0 to each ankle. First we need to transform τ_0 from the global coordinate system to a local coordinate system described by the *ground frame*. We mark all vectors in the local coordinate system with $'$. The heuristic applied is: The torque around the *x*-Axis in each ankle is approximately proportional to the force applied at that ankle. Thus:

$$\tau_{Rx}^{d'} = \alpha \tau_{0x}' \tag{4.9}$$

$$\tau_{Lx}^{d'} = (1 - \alpha) \tau_{0x}' \tag{4.10}$$

The torque around the *y*-Axis depends on the direction of the total torque τ_{0y}'. If the total torque acts in clockwise direction (negative sign), we can assume it will only be applied to the left foot. If the torque acts in anti-clockwise direction (positive sign), we assumte it will only be applied to the right foot.

$$\tau_{Ry}^{d'} = \begin{cases} \tau_{0y}', & \tau_{0y'} > 0 \\ 0, & else \end{cases} \tag{4.11}$$

$$\tau_{Ly}^{d'} = \begin{cases} \tau_{0y}', & \tau_{0y'} < 0 \\ 0, & else \end{cases} \tag{4.12}$$

We can now transform the torques form our local coordinate system to the coordinate system of the corresponding foot yielding τ_L^d and τ_R^d.

Now that we have obtained the reference torques, we can try to control the torque in each angle using the measured torques τ_R and τ_L. However since we assume a position controlled robot, the torque differences need to be translated into pose changes. There are three primary cases that need to be considered if we change the reference pose of a foot:

The foot is not in contact with the ground: Changing the reference pose will just affect the foot

The foot is in contact with the ground, but the contact is non-solid: If the foot has a soft contact surface (e.g. rubber) we can model the contact with the ground as springs that connect the ground

with the contact points on the foot. Changing the pose of the foot will relax/compress the springs and change the contact forces acoordingly.

The foot is in solid contact with the ground: Changing the reference foot pose *will not change the foot pose at all*. Instead, the pose of the rest of the robot is changed. If the foot pose is changed by the angles $\Delta\phi$ and $\Delta\theta$ all other frames of the robot will be changed by $-\Delta\phi$ and $-\Delta\theta$.

IK model <->
real robot

For a foot with a rubber surface we will start with a non-solid contact and transition to a solid contact, once the rubber is sufficiently compressed.

To get an idea how changing the pose on such a foot with rubber surface affects the torque, consider the case of rotating the foot around its lateral axis (x-Axis) in anti-clockwise direction. Since the contact with the ground is at first non-solid, we can employ the spring model. The springs at the front of the foot are compressed thus the force applied at the corresponding contact points increases. Accordingly the springs at the back are compressed less, thus the force applied to the corresponding contact points decreases. Resulting we see a increase in torque around the *x*-Axsis.

If the springs are compressed sufficiently, we can assume the contact with the floor is solid. Since the pose of the foot does not change, the increase in the joint angle in the ankle will rotate the upper body backwards. Recall the 3D-LIMP model for a moment, in that model this means our pendulum swings backwards. This will lead to an increase of the torque around the *x*-Axis in the base of the pendulum, the ankle joint.

For rotating the foot around the *y*-axis the same ideas hold.

As a result we see that additional foot rotation long the *x*- and *y*-Axis have a proportional relationship with the torque around that axis. This motivates the definition of the controller proposed by Kajita et. al. The additional rotation angles are can be calculated by the following equations:

Maybe add a
step response to
the controller

$$\Delta\dot{\phi}_i = \frac{1}{D_{ix}}(\tau_{ix}^d - \tau_{ix}) - \frac{1}{T_{ix}} \cdot \Delta\phi_i \tag{4.13}$$

$$\Delta\dot{\theta}_i = \frac{1}{D_{ix}}(\tau_{iy}^d - \tau_{iy}) - \frac{1}{T_{ix}} \cdot \Delta\theta_i \tag{4.14}$$

Where $i \in \{R, L\}$. This again utilizes the same concept of a dampening controller that was used previously for controlling the chest frame orientation. We can use the obtained angles $\Delta\phi_i$ and $\Delta\theta_i$ to compute the modified reference frames for the feet:

$$R_i^{d*} = R_i^d \cdot R_{RPY}(\Delta\phi_i, \Delta\theta_i, 0) \tag{4.15}$$

4.2.3 Foot force difference controller

In the previous section only the ankle torque were controlled to match the reference values that were derived using the ZMP distributer. However reference values for the gravitational force that each foot exerts on the ground were also obtained. These forces are not necessarily realized. Consider the case of slightly uneven ground. If the pattern assumed a flat ground, the ankle of both feet will have the same altitude. Depending on variation of floor height, that might lead to one foot not touching the ground at all. In the case of feet with rubber soles, slight variations in floor height lead to a different compression of the soles. Both cases cause a different force acting on each foot.

If we assume the mass M of the robot and the gravity vector g are correct, we know that the reference force $f_g^d = M \cdot g$ will exactly match the force in z-direction f_g exerted by the support foot in single support. Thus in single support we can guarantee that we realize our reference force. In dual support we know that $f_L^d + f_R^d = M \cdot g$. If we apply the same reasoning as above we know that $f_L^d + f_R^d = f_L + f_R$. If we can additionally make sure that $f_L^d - f_R^d = f_L - f_R$ we can deduce that $f_L^d = f_L$ and $f_R^d = f_R$. Equation 4.7 can be used to calculate the ZMP position from the applied forces and torques on the foot. If both

reference torques and reference forces on the feet are realized, that will guarantee the reference ZMP is also realized.

Since the x and y components of both $f_L^d - f_R^d$ and $f_L = f_R$ are zero we only need to control the z components. As we motivated in the beginning of this section, differences in floor height are the main cause of deviation in the force. To compensate that, the height of the ankle needs to be changed. Thus the difference in ankle height z_{ctl} was chosen to compensate the difference in forces exerted by the foot. The description of the controller again uses the concept of a dampening controller, that was used in the previous sections.

$$\dot{z}_{ctl} = \frac{1}{D_z}[(f_L^d - f_R^d) - (f_L - f_R)] - \frac{1}{T_z}z_{ctl} \tag{4.16}$$

Two methodes were proposed to realize this difference in ankle height. The first methode is straight forward change the reference position of the feet in z-direction:

$$p_R^{d*} = p_R^d + 0.5 \cdot \begin{pmatrix} 0 \\ 0 \\ z_{ctl} \end{pmatrix} \tag{4.17}$$

$$p_L^{d*} = p_L^d - 0.5 \begin{pmatrix} 0 \\ 0 \\ z_{ctl} \end{pmatrix} \tag{4.18}$$

This can lead to singularities if both legs are already fully streched, as the edge of their workspace is reached. The second methode relies on an additional rotating the pelvis link. For this approach to work, the robot needs a joint that allows rotations around the anterior axis (y-Axis) to keep the upper body uprigt. Since the robot model we used does not have this DOF, we only implemented the first approach.

4.2.4 Interaction between controllers

While each controller operate independently, their effects are highly coupled. The most important coupling exists between the chest posture controller and the ankle torque controller. Recall that in case of a solid contact with the ground the ankle torque controller will not rotate the supporting foot but rather the body of the robot. This will however change the posture of chest frame. The chest posture controller compensates that and keeps the body upright. This tight coupling makes tuning the parameters D_i and T_i of the controllers difficult, as their performance depends on the other controllers. Best results where observed when the chest posture controller was tuned independently first, disabling the other controllers. Then the foot force controllers was enabled and tuned and finally the ankle torque controller was added and tuned.

4.2.5 CoM and ZMP control

The controllers specified in the previous sections can make sure, that the ZMP that is realized tracks the ZMP that would result from a perfect execution of the input pattern. However depending on how the reference ZMP was predicted, that prediction might have already been wrong. For example the ZMP Preview Control approach uses the Table-Cart model to predict the ZMP. That prediction can deviate significantly from the real ZMP as the model simplifies the dynamics. Thus to make sure the desired ZMP is tracked acurately, the reference ZMP needs to be adapted as well.

Kajita et. al. propose a dynamic system that describes the 3D-LIMP dynamics. To model mechanical lag they introduce a parameter T_p that should specify the ZMP delay. The state-space description of the dynamic system for the x-direction is given below. As before, the description of the dynamic system for the y-direction is analogous.

$$\frac{d}{dt}\begin{pmatrix} c_x \\ \dot{c}_x \\ p_{zmp_x} \end{pmatrix} = \overbrace{\begin{pmatrix} 0 & 1 & 0 \\ \frac{g}{z_c} & 0 & -\frac{g}{z_c} \\ 0 & 0 & -\frac{1}{T_p} \end{pmatrix}}^{=:A} \cdot \begin{pmatrix} c_x \\ \dot{c}_x \\ p_{zmp_x} \end{pmatrix} + \overbrace{\begin{pmatrix} 0 \\ 0 \\ \frac{1}{T_p} \end{pmatrix}}^{=:B} u \qquad (4.19)$$

As controller a feedback controller is proposed:

$$p_x^{d*} = u = (k_1, k_2, k_3) \cdot \left[\begin{pmatrix} c_x^d \\ \dot{c}_x^d \\ p_{zmp_x}^d \end{pmatrix} - \begin{pmatrix} c_x \\ \dot{c}_x \\ p_{zmp_x} \end{pmatrix} \right] + p_{zmp_x}^d \qquad (4.20)$$

To derive the corresponding gains (k_1, k_2, k_3) pole-placement with the poles $(-13, -3, \sqrt{\frac{g}{c_z}})$ was proposed. The gains can be easily computed from the poles, A and B using predefined functions in MATLAB or similar software.

4.3 Implementation

FIXME: Needs introduction

4.3.1 Computing the inverse kinematics

While implementing the stabilizer above, a number of problems has to be solved. For one, computing the inverse kinematics proofed challenging. During walking the base of support depends on which foot is in contact with the ground. Thus the left foot will act as base and the right foot as TCP if the left foot is the support foot. The reverse is true if the right foot is the support foot. In dual support phase, we actually have two bases of support, which yields a parallel kinematic chain. SIMOX, the framework used to compute the inverse kinematics, describes the kinematic structure of a robot as a directed tree. Solving the inverse kinematics was initially only possible for sub-trees of that tree. That means it was not possible to chose base and TCP freely, but it was determined by the structure in which the kinematic model was initially described.

As a first approximation, a kinematic model with the left foot as root node was used. In the case of the right foot being the support foot, this approach leads to an increased error. Consider solving the inverse kinematics for both legs using a differential solver in two steps: First from the base (the left foot) to the pelvis, then from the pelvis to the right foot. Lets assume the IK computes a perfect solution to place the pevlis link and only achieves a small pose error of $e_\alpha = 0.1°$ in the pitch angle of the right foot. If the trajectory is execute, the right foot will achieve its target pose, since it is constrained by the ground contact. However the error in the right foot pose will effect all other frames of the robot. Assuming a offset of $v = (-0.5, 0, 1)^T m$ from the right foot to the pelvis link, we can compute the realized pelvis offset as $v' = R_y(-e_\alpha) \cdot v = (-0.49825, 0, 1.00087)^T m$ Which yields $1.76mm$ error in x-direction and $0.87mm$ error in y-direction.

To solve this SIMOX was extented by a function `cloneInversed` that can compute a kinematic structure with abitrary root placement from an existing description. To solve the parallel kinematic chain, it proofed sufficient to approximate it as a normal kinematic chain and constrain the base and TCP targets acordingly. However since the position of one foot will have small positioning errors, there will be some jitter introduced into the system. Integrating a solver for parallel kinematics might decrease some of the jitter observed in foot contact forces during dual support, as the constraint solver used for the simulation will only amplify this jitter.

4.3.2 Integration into the simulator

As was the case with the components of the pattern generator, the core of the stabilizer is implemented as part of LIBBIPEDAL. To integrate the stabilizer into the simulation, each stabilizer is implements the `TrajectoryController` interface. Currently three controllers are implemented. A controller based on the stabilizer propose by Kajita above, a simple heuristic stabilizer and a controller that just plays back the specified walking pattern. After each simulation cycle the physics engine invokes a callback in the simulator that calls the actived controllers and measurement units. The actual stabilizer loop runs with the same cycle-time as the specified reference trajectory. The computed reference joint angles and velocites are then interpolated using cubic splines. The joint values are then send to the motor controllers in SIMDYNAMICS which controlls the motors in BULLET.

> block diagramm of simulator

> Pose Stabilizer might be better than Cartesian stabilizer since we don't actually controll the foot position

4.3.3 Problems

Some problems became immediately clear when testing the stabilizer proposed by Kajita. The ground reaction forces in dual support are oscillating widly. Instead of a continous force at about $0.5 \cdot f_g$ the forces on both feet oscillate between 0 and f_g, the support foot changes in rapid successions. As outlines in section 2.5 this is a result of the constraint solver methode employed by BULLET. Subsequently the measured torques on the ankles did not follow the prediction as well. Pleae note that this is not merely sensor noise, these are the actual values used by the simulator. Even when adding mean-filters to smoothen the measured torques it was not possible to extract a meaningful control signal. Besides the sequential impulse solver newer versions of BULLET support a solver based on the Featherstone algorithm. Given the scope of this thesis, integrating that solver was out of question, thus an alternative approach to stabilizing had to be found.

4.3.4 Alternative approach

A a simple heuristic, we used the controllers proposed by Kajita as inspiration and replaced the force and torque feedback with the pose error of pelvis and feet frames respectively. The chest controller Kajita et. al. proposed for controlling the body posture where adapted to all control frames to provide a feedback on the pose error.

This yields a controller that keeps the feet pose parallel to the ground, which is important when the swing foot touches the ground. Controlling the pelvis and chest pose to follow the reference also keeps the robot upright. It should be noted that it is probably not feasible to implement this stabilizer in practice. As mentioned in section 4.2 precisely estimating the pose of a robot is not easy. While the dampening controllers can be configured to smoothen a noisy sensor signal, a high level of precision is required to ensure a correct foot posture.

Since the ZMP and CoM trajectory is not adaped, the compensation of environment disturbences is only based on a fast controller raction to leave the reference trajectory a little as possible and the stability margins the ZMP provides. However as we will discuss in the evaluation section, this simple approach is already suppprisingly resilient.

5 Push recovery

As we saw in the chapter about Stabilizers, not all disturbences can be compensated. If the disturbence reaches a certain severity, the trajectory can not be executed as planed without falling. Thus the trajectory needs to be changed radically to avoid falling. There is little hope to recover from continous heavy disturbences, as any attempt to recover will be defeated. Thus we focus on short but severe disturbences, pushes.

The most prominent methode to recover from pushes is the Capture Point. The idea is to find a point, that will guarantee that the CoM comes to a rest, if the support foot is instantanously placed there.

5.1 Capture Point

Add citation

Pratt derives the Capture Point for multiple models based on the 3D-LIPM.

- Read paper again
- Definition of capture point
- Capturebility <-> capture region
- Immediate Capture Point

5.2 Implementation

6 Results

6.1 Unstabilized walking

In this section the results of just playing back the patterns generated by the pattern generator are presented. In short, all patterns generated by the Pattern Generate are dynamically stable and realize walking without falling. However for some trajectories like walking in a circle, significant deviations can be observed.

6.1.1 Walking straight

Figure 6.1 shows the simulation of walking straight for 10 steps.

The top plot in figure 6.2 shows the desired ZMP and CoM. The actual realized ZMP, CoM and are shown in the bottom plot. For comparision the position of the TCP of both feet is shown as well. The ZMP shown is derived using the Cart-Table model, for a comparison of different methodes to derive the actual ZMP see 2.4. As you can see the realized ZMP roughly follows the desired trajectory, while the signal is rather noisy. To get an idea why the ZMP oscillates so much, consider figure 6.3. The acceleration of the CoM oscillates wildly. We believe this is caused by the the problems outlined in section 2.5 about rigid body simulation. In single support the ZMP oscillates near the boarder of the support polygone, but overall stays inside.
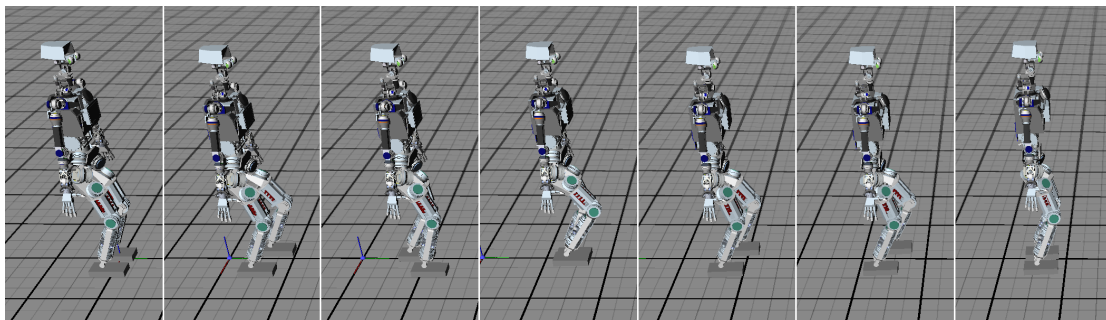

Figure 6.1: Frames of undisturbed straight walking

6.1.2 Walking in a circle

Figure 6.4 shows the simulation of walking in a circle. The robot walks in 12 steps in an arc of $180°$ and 0.5 m radius. As you can see the desired $180°$ turn is not realized completely. Due to the chest rotation following the tangent of the circle, a torque around the yaw-axis is excerted on the foot. Recall that during pattern generation we assumed that this torque is zero. Since we do not correct this disturbance the trajectory deviates significantly. However stable walking is still realized. See figure 6.5
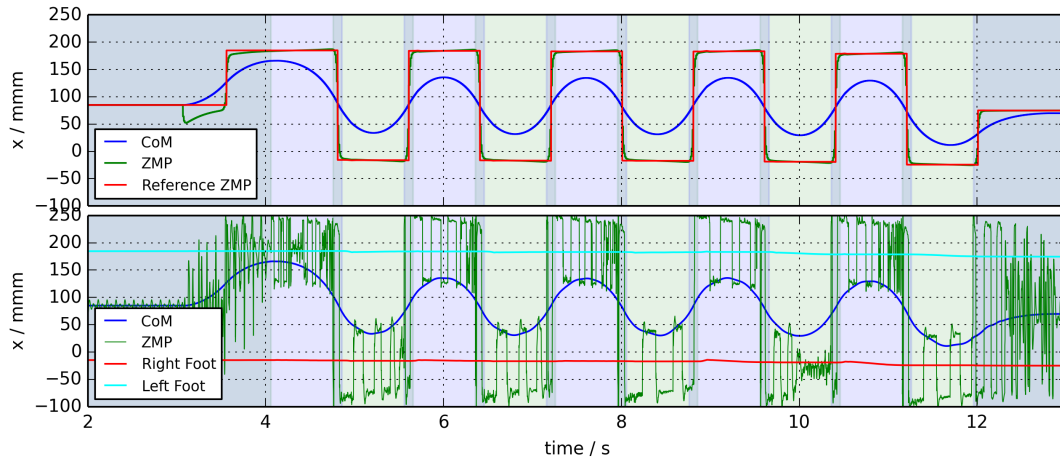
Figure 6.2: CoM and ZMP as specified by the pattern (top) and actual realized values (bottom). All coordinates in the global reference frame.
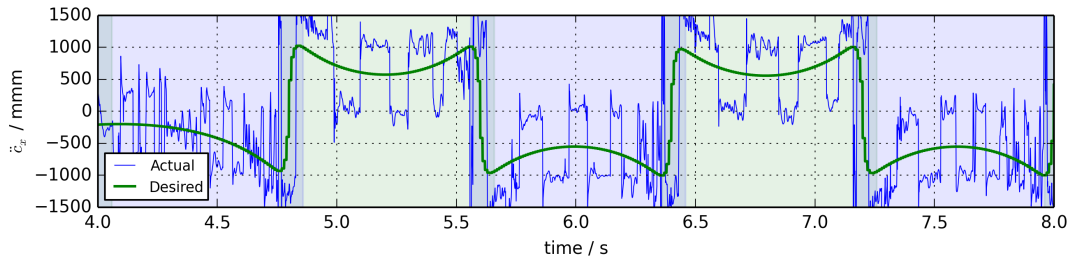

Figure 6.3: Acceleration of the CoM in *x*-direction.

6.2 Stabilized walking

In this section we present the results of using the alternative stabilizer derived from the Kajita Stabilizer. As was the case with unstabilized walking, a stable walking trajectory is realized. Smaller disturbances can be corrected to remain stable.

6.3 Undisturbed walking

Figure FIXME: ref and FIXME: ref show the realized ZMP and CoM trajectory of the same for walking straight and in a circle. As input trajectories for the stabilizer the trajectorie tested in the previous section are used.

The trajectory deviates a little more than it was the case for unstabilized walking. This is somewhat expected, since the stabilizer modifies the reference trajectory to ensure the constrains outlined in 4.3.4.

actual-zmp-straight

actual-zmp-circle
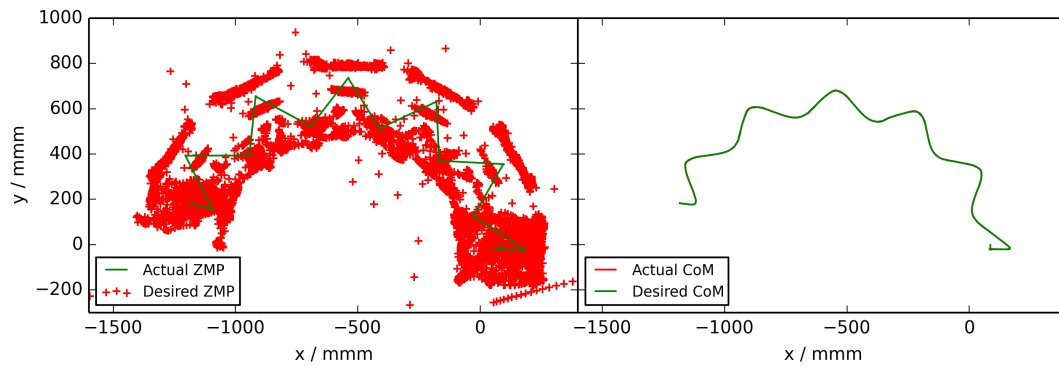
Figure 6.4: ARMAR4 walking in a half circle in 12 steps.

Figure 6.5: ZMP (left) and CoM (right) as specified by the pattern and the actually realized values.

6.4 Disturbed walking

To test the performance of the stabilizer under disturbance, we used two scenarios: A short push applied to the chest and slightly sloped ground. The results are compared with the performance of the unstabilized trajectory.

6.4.1 Push to the chest

To simulate a push, a ball with a radius of 11cm and weight of 450g (FIFA football) is shoot from 2m distance at the chest. The point of impact is denoted as red lines.

force is meaningless as we don't know the units. Maybe print ball velocity on impact

actual-zmp-stabilized actual-zmp-unstabilized

image-series

7 Conclusions

things to improve summary of work done and results

8 TODO

Todo list

6, Use different name for CoM, p will be rather used for the ZMP, maybe c?

6, reference paper

7, cite Orendurff

8, include pattern generation just based on 3D-LIPM, I don't understand how they derived the controller

12, citation needed

12, add citation

12, maybe do a formal introduction into dynamic system and the state space approach

14, insert plot

14, add citation katayama

14, block diagramm of architechture

15, table with used parameters

15, Current implementation does effectively that, but is actually a hack. Needs seperate trajectories for left/right

16, It is easy to extent this: DO IT.

16, Add timings, implement configurable preview periode

17, Maybe a more theoretical explaination?

17, Maybe doing the FK now would be better and more versatile, since we could feed normal MMM trajectories in the stabilizer

18, Make sure you can really load vanilla MMM trajectories without crashing

18, Screenshot of analysis software

19, More introduction: Most stabilizers are propritary and very robot specific.

19, add reference

19, include block digramm of controller

21, For some reason I named the class ForceDistributor, I should fix that

21, define ground frame

21, Cite kajita paper from 2005 that outlines the motivation for doing pose control

21, image with springs

22, IK model <-> real robot

22, Maybe add a step response to the controller

23, The code of that part was broken: Fix it.

23, relationship between foot force controller and other controllers

25, block diagramm of simulator

25, Pose Stabilizer might be better than Cartesian stabilizer since we don't actually controll the foot position

26, Add citation

27, Write small introduction

27, read paper about yaw compensation

27, image-series walking in a circle

28, actual-zmp-straight

28, actual-zmp-circle

29, force is meaningless as we don't know the units. Maybe print ball ve-
locity on impact

29, actual-zmp-stabilized actual-zmp-unstabilized

29, image-series

Bibliography